Morphological Studies of Poly(styrene)-*block*-poly(ethylene-*co*-butylene)-*block*-poly(methyl methacrylate) in the Composition Region of the "Knitting Pattern" Morphology§

Harald Ott,†,‡ Volker Abetz,*,‡ and Volker Altstädt†

Polymer Engineering, Technische Universität Hamburg-Harburg, Denickestrasse 15, D-21073 Hamburg, Germany, and Makromolekulare Chemie II, Universität Bayreuth, D-95440 Bayreuth, Germany

Received October 2, 2000

ABSTRACT: To investigate the stability of the knitting pattern (kp) morphology in poly(styrene)-*block*-poly(ethylene-*co*-butylene)-*block*-poly(methyl methacrylate) (SEBM) triblock copolymers, several SEBM with slightly different compositions have been synthesized. Sample preparation was done by solvent casting and melt processing techniques. Morphological investigations using transmission electron microscopy (TEM) on films cast from chloroform revealed that several polymers exhibited the kp morphology. Polymers with a higher poly(styrene) content and the same amount of poly(ethylene-*co*-butylene) as the kp polymers exhibited predominantly a lamellar morphology from chloroform cast films. Symmetric SEBM polymers with a decreased midblock content in films from chloroform resulted in a cylinder-between-lamellae (lc) morphology. Melt processed samples exhibited a predominantly co-continuous-like structure with a mixture of layerlike and cylindrical poly(ethylene-*co*-butylene) microphases between poly(styrene) and poly(methyl methacrylate). Samples that have been cast from chloroform prior to compression molding displayed predominantly the kp morphology. Additional morphological investigations on samples cast from toluene and roll-cast from chloroform were conducted, which lead to some features of the kp morphology.

Introduction

Microphase separated ABC triblock copolymers are well-known for their rich morphological diversity due to their larger number of independent compositional and segmental interaction parameters as compared to diblock copolymers. A group of triblock copolymers that have been investigated[1,2] with regard to their morphological behavior consists of poly(styrene)-*block*-poly(butadiene)-*block*-poly(methyl methacrylate) (SBM) and their hydrogenated analogues poly(styrene)-*block*-poly(ethylene-*co*-butylene)-*block*-poly(methyl methacrylate) (SEBM).[3,4]

Among the most striking structures found in these systems were the helical (hel)[3,5] and the knitting pattern (kp) morphology.[6,7] The kp morphology (Figure 1) was found to have an orthorhombic symmetry. It was only found in a chloroform cast SEBM triblock copolymer composed of 35 wt % poly(styrene), 27 wt % poly(ethylene-*co*-butylene), and 38 wt % poly(methyl methacrylate). Casting from other solvents like toluene lead to a predominantly lamellar morphology. It was speculated before that the kp morphology could be an intermediate between two lamellar morphologies: one lamellar morphology contains lamellae of all three components (ll morphology), while in the other the outer blocks form lamellae embedding cylinders of the midblock at their common interface (lc morphology).[6] While the kp morphology was never observed in pure SBM triblock copolymers, it could be obtained by blending of two SBM triblock copolymers having these different lamellar morphologies via solvent casting from chloroform.[8]

In this contribution we wish to investigate the following questions related to SEBM triblock copolymers: (i) in which composition region can this morphology be obtained, and (ii) is it possible to obtain this morphology besides casting from $CHCl_3$ solution also by other processing techniques like roll casting or melt processing?

Experimental Section

Synthesis of SBM and SEBM Block Copolymers. The synthesis of SBM was done by sequential living anionic polymerization of styrene, butadiene, and methyl methacrylate in tetrahydrofuran containing lithium alkoxides. The polymerization was initiated with *sec*-butyllithium. Details are published elsewhere.[9] SEBM was obtained after hydrogenation at 50 °C of SBM in butanone with 90 bar hydrogen pressure and Wilkinson's catalyst.

Table 1 summarizes the composition and molecular weight of the synthesized block copolymers. The molecular weights were determined from a PS precursor by size exclusion chromatography (calibrated to PS standards) and ^{1}H NMR spectroscopy of the final triblock copolymers. The volume fractions ϕ_i were obtained using the weight fractions obtained by ^{1}H NMR and the bulk densities of PS (1.05 g/cm^3), PB (0.96 g/cm^3), and PMMA (1.15 g/cm^3).[10] Subscript numbers indicate the weight percentage of the corresponding block, and the superscript numbers give the number-average molecular weight in kg/mol.

Sample Preparation by Solvent Casting. Films of approximately 1 mm thickness were obtained by slowly evaporating a corresponding polymer solution in chloroform or toluene over a period of 2−3 weeks in planar Petri dishes. The films were removed from the Petri dishes and dried in vacuo for 2 days. Subsequently, the samples were annealed at 170 °C in a vacuum for approximately 6 h. Previous studies revealed no significant cross-linking reactions under these conditions.

Sample Preparation by Melt Processing. The precipitated and subsequently dried SEBM polymers were compres-

† Technische Universität Hamburg-Harburg.
‡ Universität Bayreuth.
§ In memoriam Prof. Dr. Reimund Stadler.

10.1021/ma0017079 CCC: $20.00
Published on Web 02/23/2001

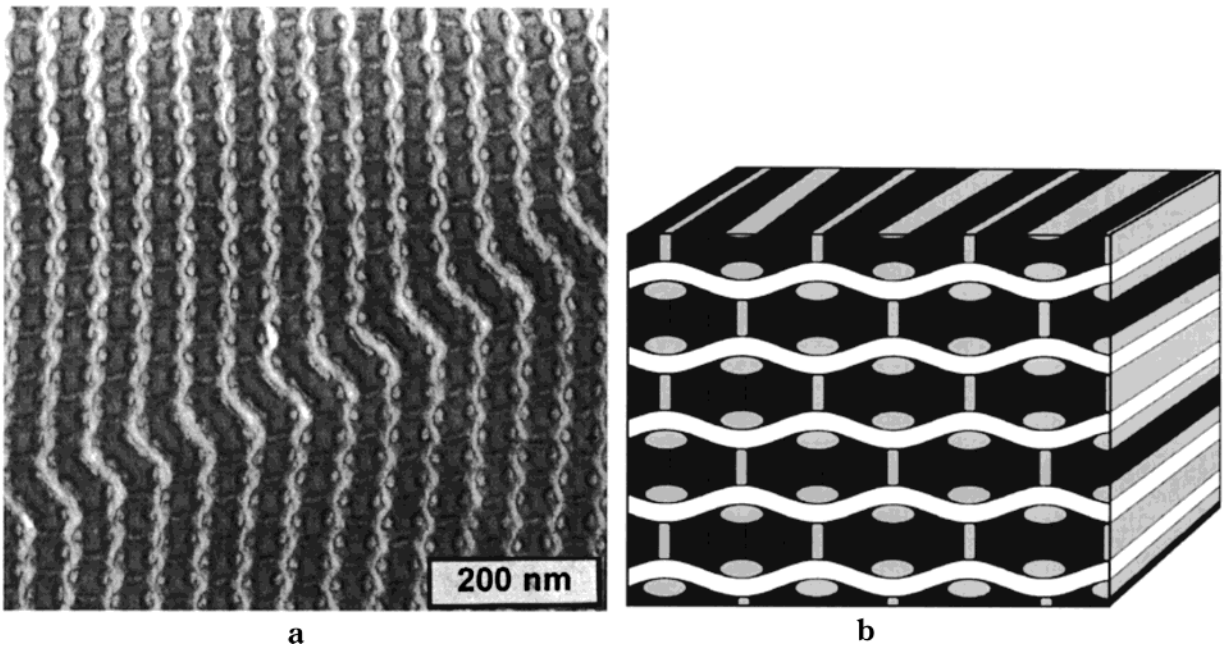

Figure 1. (a) Transmission electron micrograph of $S_{35}EB_{27}M_{38}^{115}$ stained with RuO_4; annealed film cast from chloroform. (b) Schematic representation of the kp morphology.

Table 1. Characteristics of SEBM Triblock Copolymers (Error of M_n, ⩽8%; Error of Composition, ⩽5%)

polymer	area	M_w/M_n	ϕ_{PS}	ϕ_{PEB}	ϕ_{PMMA}	M_n [kg/mol]
$S_{35}EB_{27}M_{38}^{115}$	A	1.09	0.35	0.30	0.35	115
$S_{36}EB_{29}M_{35}^{123}$	A	1.04	0.36	0.32	0.32	123
$S_{34}EB_{28}M_{38}^{101}$	A	1.04	0.34	0.31	0.35	101
$S_{37}EB_{27}M_{36}^{119}$	A	1.05	0.37	0.30	0.33	119
$S_{34}EB_{30}M_{36}^{74}$	A	1.06	0.34	0.33	0.33	74
$S_{42}EB_{27}M_{31}^{92}$	B	1.02	0.42	0.30	0.28	92
$S_{40}EB_{29}M_{31}^{89}$	B	1.03	0.40	0.32	0.28	89
$S_{42}EB_{28}M_{31}^{73}$	B	1.04	0.42	0.30	0.28	73
$S_{42}EB_{21}M_{37}^{91}$	C	1.03	0.43	0.23	0.34	91
$S_{38}EB_{24}M_{38}^{114}$	C	1.04	0.38	0.27	0.35	114
$S_{30}EB_{27}M_{43}^{121}$	D	1.05	0.30	0.30	0.40	121

sion molded between 220 and 240 °C for 25−45 min and cooled to room temperature under pressure. Samples that were solvent cast prior to melt processing were compression molded at 180 °C for 20 min. Melt processing utilizing a corotating twin-screw microcompounder (DSM, Netherlands) was done by melt mixing the polymers for 10 min at 200−220 °C followed by an extrusion process through a 1 mm dye.

Sample Preparation by Roll Casting. One SEBM polymer sample was prepared on a roll caster[11] from a concentrated solution (15 wt %) in chloroform at around 25 rpm for 10 min.

Transmission Electron Microscopy. TEM was performed on a Philips EM 400 at 100 kV in the bright field mode. Ultrathin sections of the samples were obtained with a Leica UCT Ultramicrotome using a diamond knife at room temperature. The sections (approximately 60 nm thick) were transferred to guilded grids and subsequently stained with gaseous RuO_4 prepared from $RuCl_3$ and NaOCl(aq). RuO_4 stains the poly(styrene) (PS) phases dark gray as well as the interface between the components.

Results and Discussion

The synthesized SEBM polymers are summarized in Figure 2. Depending on the composition, four areas can be distinguished: area A consists of five nearly symmetrical SEBM polymers close to the composition found earlier for the kp morphology. Polymers in area B have a higher poly(styrene) (PS) content but the same amount of midblock elastomer as those in group A. Area C has a decreased midblock content. Area D contains a polymer with an increased poly(methyl methacrylate) (PMMA) content.

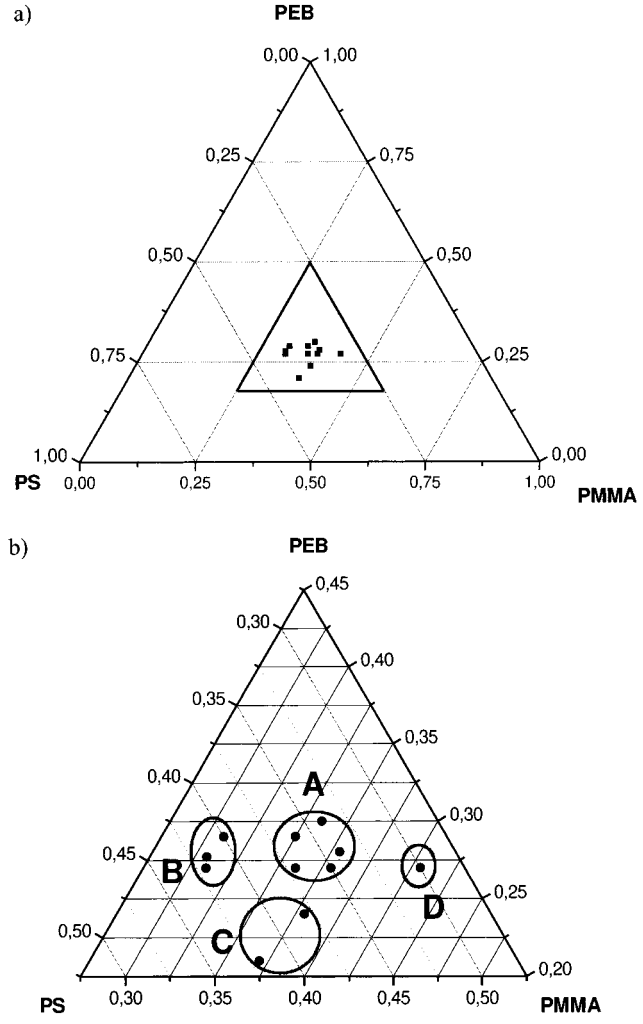

Figure 2. Ternary composition diagram (wt %) with a close-up view of synthesized SEBM triblock copolymers.

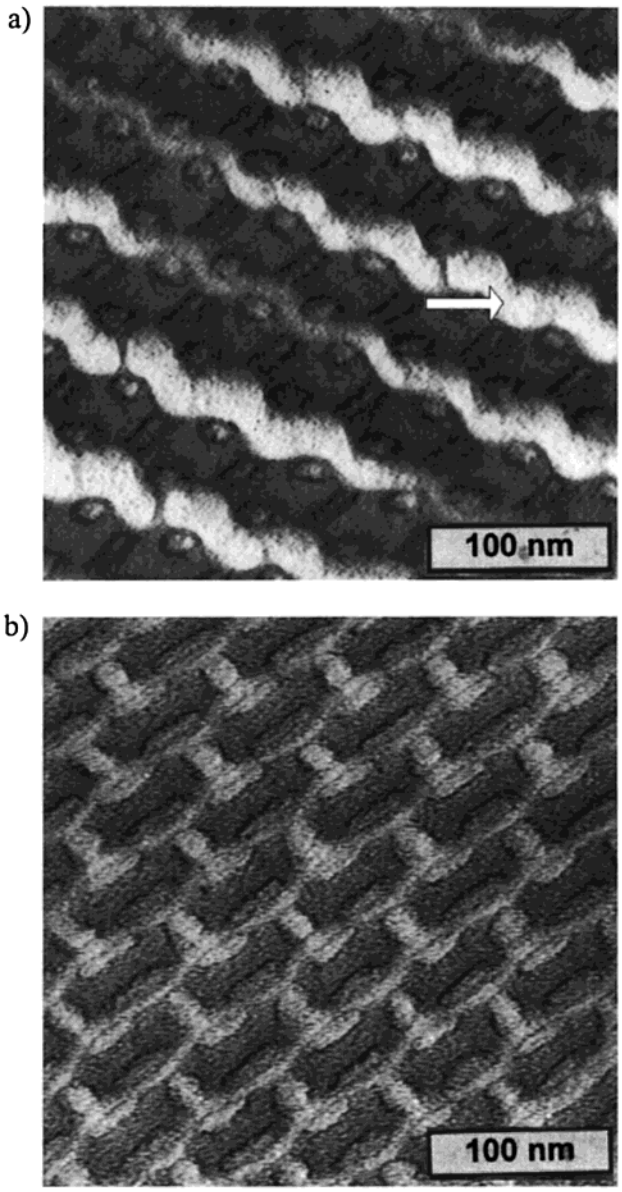

Figure 3. Transmission electron micrograph of different SEBM block copolymers; all samples cast from chloroform and stained with RuO_4: (a) $S_{36}EB_{29}M_{35}^{123}$, arrow: damaged PMMA area due to electron beam degradation; (b) $S_{34}EB_{28}M_{38}^{101}$.

Morphology of Solvent Cast Samples. Four SEBM samples from area A except the one with the highest midblock content displayed the kp morphology in the TEM from chloroform cast films (Figure 3a,b). The PS microphase appears dark gray (RuO_4 staining) in the TEM micrographs. The poly(ethylene-*co*-butylene) (PEB) cylinders are visible due to preferred staining in the interface region. The poly(methyl methacrylate) (PMMA) forms the typical sinusoidal lamellae.

Some white areas between the PS microphases (arrow in Figure 3a) can be associated with electron beam degradation of PMMA, causing a weakening and subsequent failure of the PMMA lamellae. A deviation of the kp morphology can be found in the $S_{34}EB_{28}M_{38}^{101}$ film (Figure 3b): the curvature between PMMA and PS seems to be much less pronounced than in the previous samples. A possible explanation for this behavior is a different projection of the kp morphology in Figure 3b as compared to Figure 3a. This becomes evident in another picture of $S_{34}EB_{28}M_{38}^{101}$ taken at lower magnification (Figure 4). Here a grain boundary between two differently oriented domains is visible. While at the lower left part the curvature of the microphase boundary between PS and PMMA seems to be less pronounced and all the PEB cylinders seem to have ellipsoidal cross sections, the upper right part of Figure 4 shows a stronger curved interphase between PS and PMMA and circular shaped cross sections of the nonbridging PEB cylinders.

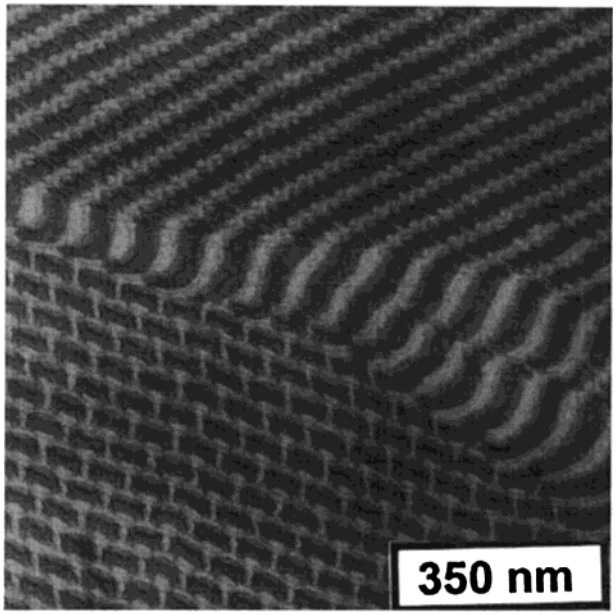

Figure 4. Transmission electron micrograph of $S_{34}EB_{28}M_{38}^{101}$ cast from chloroform and stained with RuO_4 showing two different projections of the kp morphology.

The $S_{34}EB_{30}M_{36}^{74}$ sample having the highest midblock content displayed PEB cylinders which are partially connected due to the higher volume fraction (arrow in Figure 5a). This sample marks the upper level for the midblock content necessary for the formation of the kp morphology.

All SEBM polymers of region B (higher PS content) had a lamellar (ll) morphology except for one (Figure 5b) which displayed some tendencies toward a cylinder-between-lamellae (lc) morphology. No tendencies toward the kp morphology could be found in those samples, which is reasonable since the penetration of the midblock PEB through the PS is hindered by the relative increase of the PS lamellae thickness.

SEBM samples from region C (low midblock content) had a cylinder-between-lamellae (lc) morphology (Figure 5c). The absence of the kp morphology in this composition area can be ascribed to the relative increase in PS lamellae thickness in combination with a relative decrease of the midblock chain length which again hinders the penetration of the PS microphase.

The SEBM polymer from area D (higher PMMA content) developed a kp morphology (Figure 5d) like the polymers from area A. The smaller dimensions of the PS domains in this case seem to favor the penetration of the PS by PEB cylinders. Thus, SEBM triblock copolymers with an even larger amount of PMMA may result in a kp morphology before a further increase of the PMMA content finally leads to another morphology with a PMMA matrix, such as core−shell cylinders (cic) or a cylinder-at-cylinder (cac) morphology.[3]

Roll-casting experiments with an SEBM polymer from region A dissolved in chloroform yielded an irregular

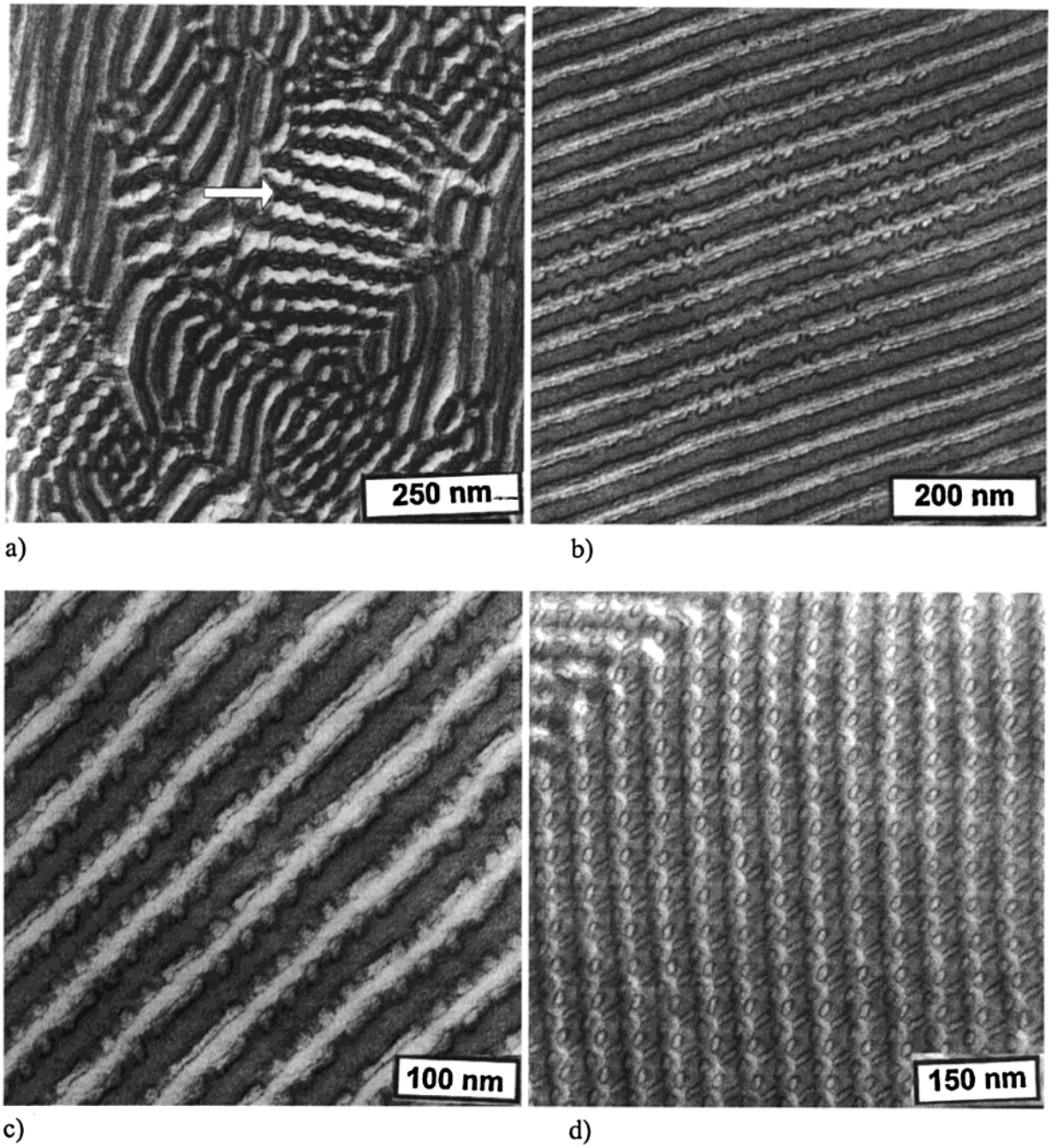

Figure 5. Transmission electron micrograph of different SEBM block copolymers; all samples cast from chloroform and stained with RuO_4: (a) $S_{34}EB_{30}M_{36}^{74}$, arrow: connected cylindrical domains; (b) $S_{40}EB_{29}M_{31}^{89}$; (c) $S_{38}EB_{24}M_{38}^{114}$; (d) $S_{30}EB_{27}M_{43}^{121}$.

morphological structure (Figure 6a) with PEB cylinders parallel aligned to the direction of flow. The cylinders were found to be predominantly bridging through the PS microphase (Figure 6b, top)—a behavior known from the kp morphology except that the cylinders located along the PS/PMMA interface were underrepresented. A possible reason for this structural feature could be the fast evaporation process favoring an arrangement closer to the more disordered situation in the concentrated solution. In the early stage of evaporation it can be assumed that the PS and PMMA chains are mixed to a certain extent. During further solvent evaporation (Figure 6b, middle and bottom) the two end blocks get more and more phase separated. For the roll-cast samples the period of time allowed for that process is reduced compared to the slow evaporation during normal film preparation.

PEB cylinders penetrating the PS do have four neighboring domains with a strong curvature of the PS microphase. In this case for example a PS chain located in an area that will transform into a PMMA microphase can relocate itself by relatively small rearrangements to a developing PS microphase as indicated by the smaller angle in Figure 6b. For PEB cylinders which will be located along the PS/PMMA interface there are only two neighboring microphases with a moderate curvature. Here the distances for rearrangements are larger, and thus the formation of this structure should require more time. Therefore, the formation of PEB cylinders bridging through the PS should be more favored.

Films cast from toluene resulted in different morphologies for SEBM polymers from area A (kp region). Predominantly distorted ll structures with areas that

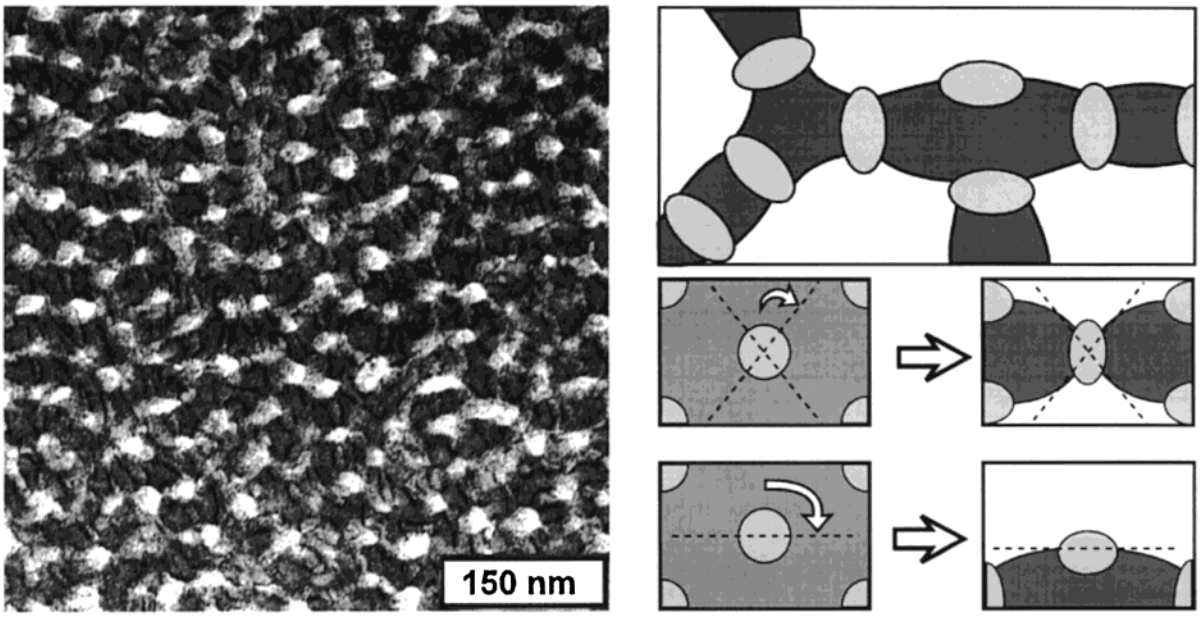

Figure 6. (a) Transmission electron micrograph of $S_{36}EB_{29}M_{35}^{123}$; roll-cast from chloroform solution and stained with RuO_4; direction of flow field perpendicular to viewing plane; (b) schematic representation of the arrangement of PEB midblock component (top), development of different PEB cylinders (bottom).

showed tendencies toward the kp morphology were found in agreement with previous work.[12] This difference can be attributed to the influence of the solvent upon morphology development.[13,14] Since toluene is a better solvent for the PEB as compared to the other blocks, the PEB domains are swollen more than the outer blocks at the point where the morphology is formed. This leads to lamellar arrangements of the midblock.

Melt Processed Samples. SEBM polymers from area A did not exhibit the kp morphology if melt processed using a twin-screw microcompounder (Figure 7a,b). The morphologies found at different screw speeds resemble co-continuous structures with PEB layers between the PS and PMMA microphases instead of cylinders. Only small distorted areas showed some cylindrical PEB microphases. At higher screw speeds the morphology becomes more irregular.

In contrast to this morphology, a spherical morphology (spheres-on-spheres, sos) has been reported[4] to show the same morphology after solvent casting and melt processing, indicating that a spherical structure is not that sensitive to shear deformations than the rather complex kp morphology.

To lower the influence of shear forces during processing, a polymer from area C (low midblock content) was melt pressed (Figure 7c). The obtained morphology resembles those from the microcompounder experiments except that almost no distorted areas with cylindrical PEB domains could be found.

Samples from area C that have been melt pressed at 220 °C for a shorter period of time (25 min) contained more cylindrical than layerlike PEB domains. An explanation for this behavior is that even the neat powder has experienced a solvent influence during the synthesis and the workup procedure. THF and butanone are even poorer solvents for the PEB midblock than chloroform. Since DSC results[15] of powder samples (precipitated from butanone solution) revealed a microphase separated midblock during the first heating cycle, it is reasonable to assume that a discontinuous nonlamellar PEB microphase already existed prior to melt processing.

The longer the melt processing conditions are applied, the more layerlike PEB domains form. This observed tendency can be interpreted as an evidence for the metastable nature of the kp morphology since a layerlike structure seems to be more stable at least at elevated temperatures even for those block copolymers with a lower PEB content (area C).

The fact that for longer processing durations even at low midblock contents the PEB forms layers instead of cylinders clearly shows the influence of the processing on the morphology development. Since samples of the corresponding block copolymer prepared by solvent casting using chloroform exhibited the lc morphology (see Figure 5c), it can be assumed that the kp morphology cannot be achieved via means of melt processing by further lowering the PEB content. This would certainly lead to a point where PEB arranges into cylindrical domains, but the relative chain lengths of PS and PEB would prevent the PEB from penetrating through the PS microphase.

A combination of chloroform casting and compression molding was tried to obtain the kp morphology suitable for mechanical tests (which will be reported elsewhere[16]). The kp morphology is the predominant structure (Figure 8a). Between the areas showing the typical kp projection a "lamella-like" structure is found, which most likely corresponds to a parallel projection along cylindrical axes of PEB domains, as shown in Figure 8b.

However, also the ll morphology was found after these preparation conditions in one of the samples of area A ($S_{34}EB_{28}M_{38}^{101}$, not shown). The PEB lamellae can be generated by shear forces during compression molding.

Stability and Development of the kp Morphology. By putting the different results together, it can be concluded that the kp morphology is a metastable structure, the formation of which is promoted by the

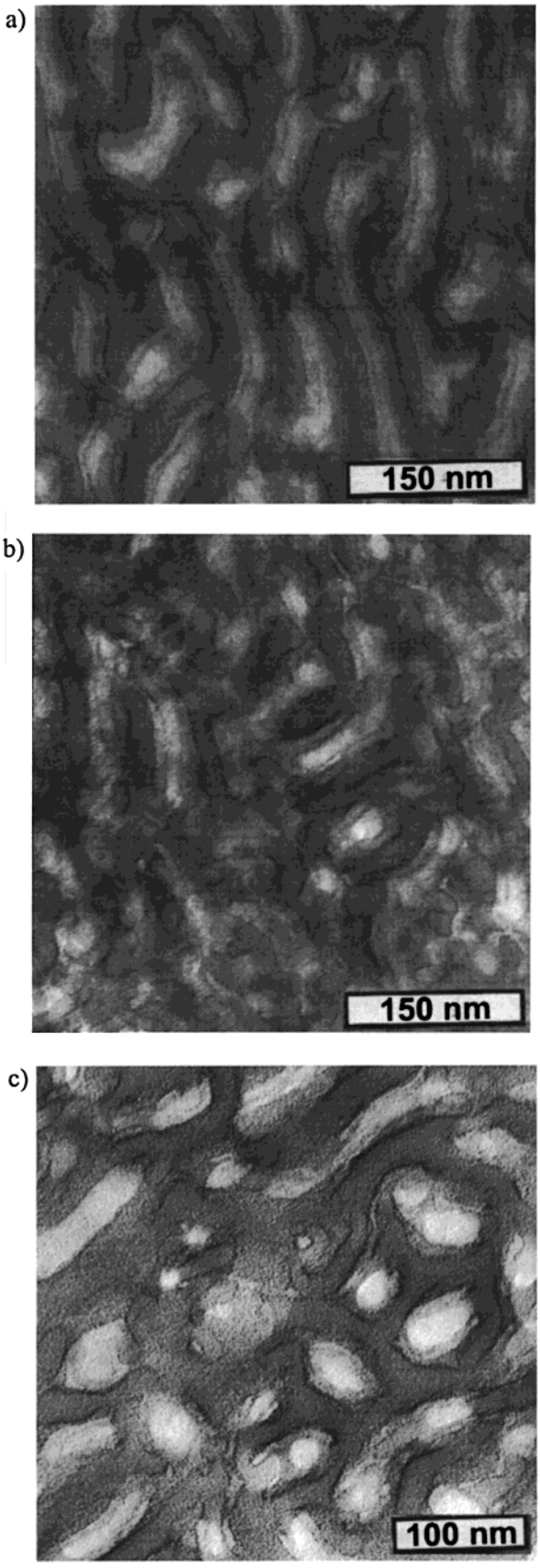

Figure 7. Transmission electron micrograph of different melt processed SEBM block copolymers; all samples stained with RuO_4: (a) $S_{35}EB_{27}M_{38}^{115}$ twin-screw compounder 240 °C, 20 rpm (10 min); (b) $S_{35}EB_{27}M_{38}^{115}$ twin-screw compounder 240 °C, 80 rpm (10 min); (c) $S_{42}EB_{21}M_{37}^{91}$ compression molded 240 °C (45 min).

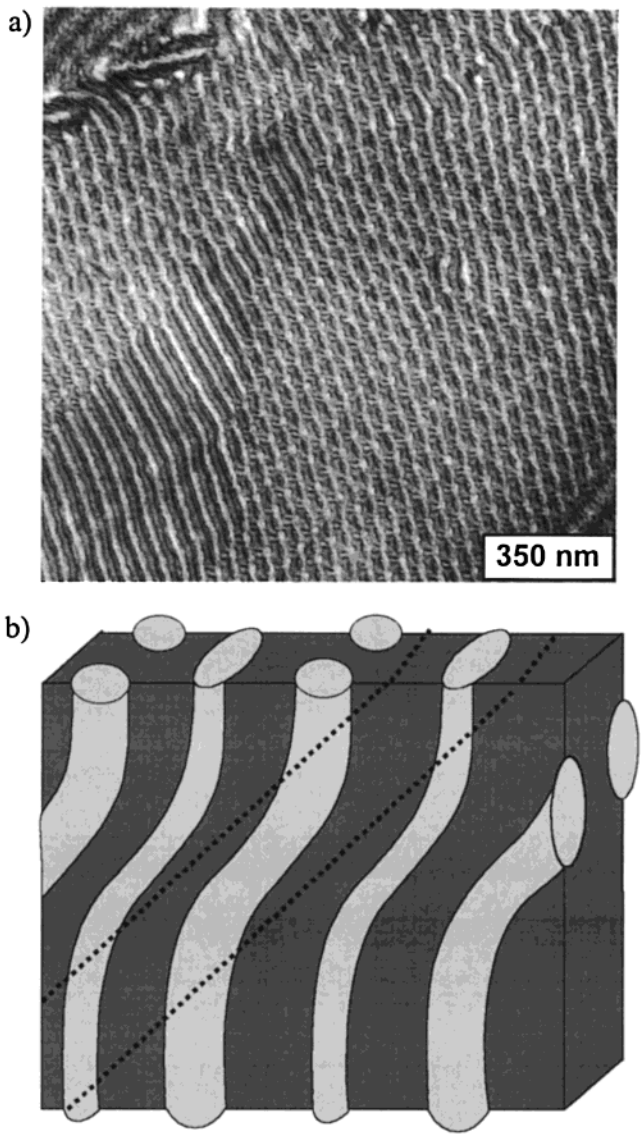

Figure 8. (a) $S_{35}EB_{27}M_{38}^{115}$ compression molded film cast from chloroform, 180 °C. (b) Scheme of an orientational defect (only PS (dark) and PEB (gray) are shown).

influence of solvents. Especially those that are poorer solvents for the PEB midblock compared to PS and PMMA result in agglomerated midblock domains needed to develop typical features of the kp morphology.

The midblock cylinders bridging through the PS are stabilizing a developed kp morphology since they contain entangled chains trapped in different microphases (Figure 9a). Transformation of those cylinders into layer domains similar to an ll morphology would require complete blocks to be pulled through incompatible phases—a process which is strongly activated.[17,18] Other entanglements may also be present (Figure 9b,c), but their stabilizing influence is less pronounced.

Concerning the influence of the solvent on the development of the kp morphology, the following model is proposed. It is assumed that at a certain stage during the solvent evaporation the PEB forms agglomerated cylinder-like domains containing a small amount of solvent molecules. These cylinders are surrounded by a uniform matrix of PS and PMMA swollen with a higher amount of solvent. In an idealized structure the cylinders are hexagonally distributed (Figure 10, top row). As the solvent evaporation continues, the matrix

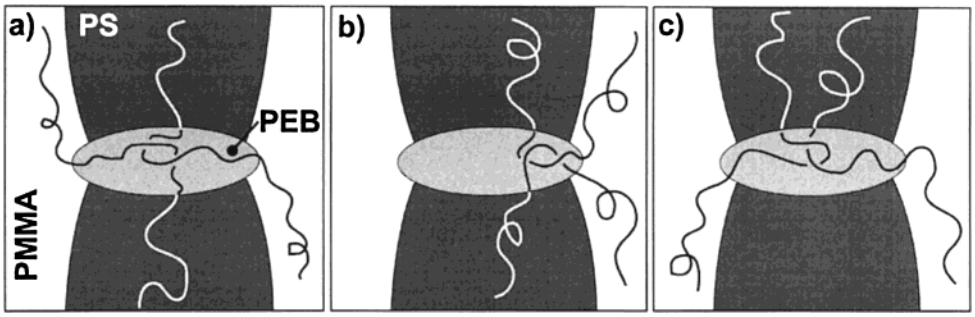

Figure 9. Different types of entanglements in PEB cylinders bridging through PS.

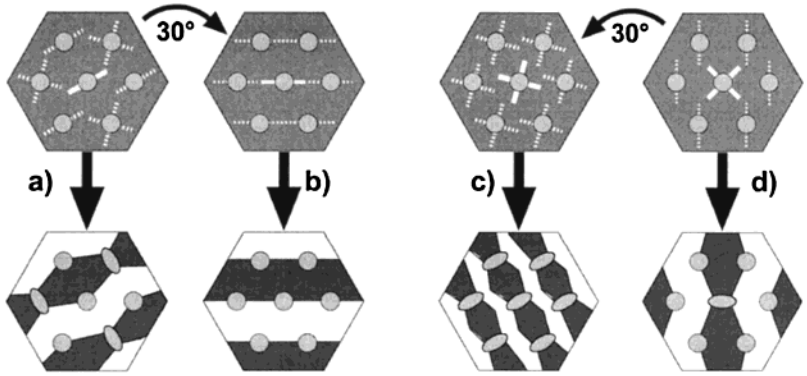

Figure 10. Schemes of the formation of different morphologies (PS: dark, PEB: light gray, PMMA: white, PS/PMMA/solvent: dark gray).

starts to undergo a microphase separation between the PS and PMMA end blocks (Figure 10, bottom row).

During the microphase separation the separation around one PEB cylinder influences the orientation of the microphase separation around adjacent cylinders since the system tries to minimize interfacial areas. The cylinders at the center of each scheme represent those cylinders that influence the microphase separation of PS and PMMA around the neighboring cylinders in an idealized manner.

The model allows the formation of four domains of the end blocks (two PS and two PMMA domains, results in bridging PEB cylinders) as well as two domains (lc-type PEB cylinders). For symmetry reasons different orientations rotated 30° left or right are possible. This leads to four structures, of which two are the kp morphology (Figure 10a,d). Features of the other idealized structures could be found in the roll-cast sample (Figure 10c) as well as in defect structures in the kp morphology (Figure 10b, also compare with 30° kink with lc PEB cylinders in Figure 1).

Conclusions

The morphological investigations of films cast from chloroform have shown that the kp morphology is reproducible within a certain composition area: the PEB content has to be about 27−29 wt %. Above these values the cylinders formed connected domains until finally a lamellar (ll) morphology developed. A decreased PEB content lead to a cylinder-between-lamellae (lc) morphology. The kp morphology requires an end block composition which reaches from symmetric end blocks to PMMA-enriched SEBM polymers. A PS increase resulted in lamellar (ll) morphologies. The maximum allowed PMMA content for the kp morphology is above 43 wt % but was not exactly investigated. An important aspect is the PS/PEB ratio because it determines if the midblock can bridge through the PS microphase.

SEBMs cast from toluene solution revealed only tendencies toward the kp morphology. This can be interpreted by looking at the structural features of the kp morphology as not only a unique phenomenon of a kinetic effect of the sample preparation but also a universal principle how a multiphase system arranges itself for a given set of volume fractions and interaction parameters.

A comparison of melt processing experiments and the solvent cast samples revealed the fundamental influence of the solvent upon morphology development. It was not possible to erase the influence of former treatment, i.e., solvent casting, of the samples. Since chloroform is the least favorable solvent for the PEB in this system, it favored a cylindrical agglomeration of the PEB during the solvent evaporation. During melt processing the arrangement of the midblock into cylinder-like microphases is more pronounced at shorter processing times. Longer processing times or higher shear forces (compounder) led to predominantly layerlike PEB domains. This different behavior under solvent-free conditions is an indication that the kp morphology for the given systems is not an equilibrium structure in a thermodynamic sense but a physically pinned structure of a four-component system including chloroform.

The method using solvent casting and subsequent compression molding revealed the difficulty to thermally erase the morphological history of the sample, since it was possible to preserve the kp morphology during compression molding. A model for the development of the kp morphology has been proposed which explains different structural features found in the TEM micrographs.

Acknowledgment. The authors are indebted to Reimund Stadler for many stimulating discussions prior to this work. Financial support of the Deutsche Forschungsgemeinschaft (SFB 371 and SFB 481) and the

Bayreuther Institut für Makromolekülforschung (BIMF) is gratefully acknowledged.

References and Notes

(1) Stadler, R.; Auschra, C.; Beckmann, J.; Krappe, U.; Voigt-Martin, I.; Leibler, L. *Macromolecules* **1995**, *28*, 3080.
(2) Bates, F. S.; Fredrickson, G. H. *Phys. Today* **1999**, *5*, 32.
(3) Breiner, U.; Krappe, U.; Abetz, V.; Stadler, R. *Macromol. Chem. Phys.* **1997**, *198*, 1051.
(4) Breiner, U.; Krappe, U.; Jakob, T.; Abetz, V.; Stadler, R. *Polym. Bull.* **1998**, *40*, 219.
(5) Krappe, U.; Stadler, R.; Voigt-Martin, I. *Macromolecules* **1995**, *28*, 4458.
(6) Breiner, U.; Krappe, U.; Stadler, R. *Macromol. Rapid Commun.* **1996**, *17*, 567.
(7) Breiner, U.; Krappe, U.; Thomas, E. L.; Stadler, R. *Macromolecules* **1998**, *31*, 135.
(8) Goldacker, T.; Abetz, V. *Macromol. Rapid Commun.* **1999**, *20*, 415.
(9) Auschra, C.; Stadler, R. *Polym. Bull.* **1993**, *30*, 257.
(10) Brandrup, J., Immergut, E. H., Eds.; *Polymer Handbook*, 4th ed.; J. Wiley & Sons: New York, 1999.
(11) Albalak, R. J.; Thomas, E. L. *J. Polym. Sci., Polym. Phys. Ed.* **1993**, *31*, 37.
(12) Breiner, U. Doctoral Dissertation, Johannes Gutenberg Universität, Mainz, 1996.
(13) Isono, Y.; Tanisugi, H.; Endo, K.; Fujimoto, T.; Hasegawa, H.; Hashimoto, T.; Kawai, H. *Macromolecules* **1983**, *16*, 5.
(14) Funaki, Y.; Kumano, K.; Nakao, T.; Jinnai, H.; Yoshida, H.; Kimishima, K.; Tsutsumi, K.; Hirokawa, Y.; Hashimoto, T. *Polymer* **1999**, *40*, 7147.
(15) Ott, H. Doctoral Thesis, in preparation.
(16) Ott, H.; Altstädt, V.; Abetz, V. Manuscript in preparation.
(17) Rubinstein, M.; Obukhov, S. P. *Macromolecules* **1993**, *26*, 1740.
(18) Fredrickson, G. H.; Bates, F. S. *Annu. Rev. Mater. Sci.* **1996**, *26*, 501.

MA0017079